THE JOURNAL OF PHYSICAL CHEMISTRY LETTERS
A JOURNAL OF THE AMERICAN CHEMICAL SOCIETY

pubs.acs.org/JPCL

Letter

Ultrafast Excitation Energy Transfer Dynamics in the LHCII−CP29−CP24 Subdomain of Plant Photosystem II

Thanh Nhut Do, Hoang Long Nguyen, Parveen Akhtar, Kai Zhong, Thomas L. C. Jansen, Jasper Knoester, Stefano Caffarri, Petar H. Lambrev,* and Howe-Siang Tan*

Cite This: *J. Phys. Chem. Lett.* 2022, 13, 4263−4271

Read Online

ACCESS | Metrics & More | Article Recommendations | Supporting Information

ABSTRACT: We measure the two-dimensional electronic spectra of the LHCII(M)−CP29−CP24 complex in photosystem II (PSII) and provide the first study of the ultrafast excitation energy transfer (EET) processes of an asymmetric and native light-harvesting assembly of the antenna of PSII. With comparisons to LHCII, we observe faster energy equilibrations in the intermediate levels of the LHCII(M)−CP29−CP24 complex at 662 and 670 nm. Notably, the putative "bottleneck" states in LHCII exhibit faster effective dynamics in the LHCII(M)−CP24−CP29 complex, with the average lifetime shortening from 2.5 ps in LHCII to 1.2 ps in the bigger assembly. The observations are supported by high-level structure-based calculations, and the accelerated dynamics can be attributed to the structural change of LHCII(M) in the bigger complex. This study shows that the biological functioning structures of the complexes are important to understand the overall EET dynamics of the PSII supercomplex.

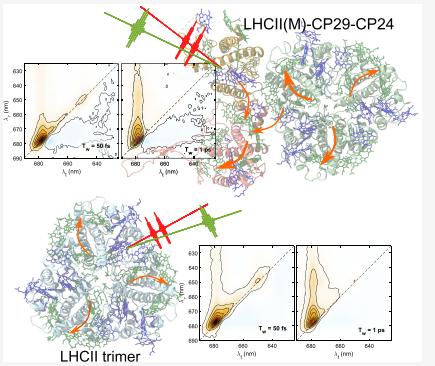

Photosystem II (PSII) is an integral component of the photosynthetic machinery in plants that fuels almost all lives and bioactivities on Earth. PSII uses the solar energy harvested by chlorophylls (Chls) and carotenoids to catalyze the oxidation of water, generating oxygen as a byproduct.[1] PSII relies on a peripheral antenna array of light-harvesting complex II (LHCII) to capture sunlight and transfer the excitation energy to the core complex and the reaction center. Higher plant PSII supercomplexes (PSII-SCs) with a different LHCII organization have been purified depending upon species and purification conditions.[2−7] The apoproteins of the PSII antennas are encoded by six nuclear genes named *Lhcb1*−*Lhcb6*.[8] The Lhcb proteins fold with the associated pigments, Chls *a* and *b* for light-harvesting function, and different carotenoids for structural stabilization and photoprotection.[9,10] In the largest stable PSII-SC purified from angiosperms (see Figure 1a), the dimeric PSII core is associated with four LHCII trimers composed of different combinations of Lhcb1−3 proteins,[4,9,11] which are connected to the PSII core via the monomeric complexes Lhcb4, Lhcb5, and Lhcb6, also named CP29, CP26, and CP24, respectively. Two of the LHCII trimers, denoted S (dark gray color in Figure 1a), are strongly bound to the core complex, while the other two, denoted M (light green color in Figure 1a) are moderately bound and can be dissociated from the PSII-SC as a pentamer composed of LHCII(M)−CP29−CP24.[3,12]

To understand the high quantum efficiency and ability of PSII to balance between light harvesting and photoprotection, detailed knowledge of how excitation energy flows within and between different subunits is necessary. The challenging goal of mapping the ultrafast dynamics of this process necessitates the coordination of structural, theoretical, and spectroscopic data.[9] Ultrafast two-dimensional electronic spectroscopy (2DES) is well-suited to reveal the excitonic couplings between the densely packed pigments and the excitation energy transfer (EET) network in highly complex photosynthetic systems.[13−15] 2DES has been successfully applied to resolve the excitation energy flow in the whole photosynthetic apparatus of green sulfur bacteria from the chlorosome to the reaction center via the Fenna−Matthews−Olson protein.[16] For PSII-SC, 2DES has been applied to certain separated components of the PSII-SC, including the PSII core complex,[17] the reaction center,[18−23] LHCII trimers,[24−31] and CP29.[32] Apart from mapping out the EET within each complex, it is also crucial to track the energy transfer between complexes. Hitherto, no 2DES studies have been deployed to resolve the EET dynamics between the various components of the PSII-SC. The currently available data about intercomponent EET in PSII complexes are restricted to a time-resolved fluorescence study that recovers a coarse-grain picture of the EET and charge separation dynamics.[2] In this Letter, we investigate the EET dynamics of the LHCII(M)−CP29−CP24 complex (henceforth referred to as the M−CP_2 complex) and compare it to the EET dynamics of detergent-solubilized LHCII trimers at 80 K. The M−CP_2 complex can serve as the

Received: January 21, 2022
Accepted: May 2, 2022
Published: May 6, 2022

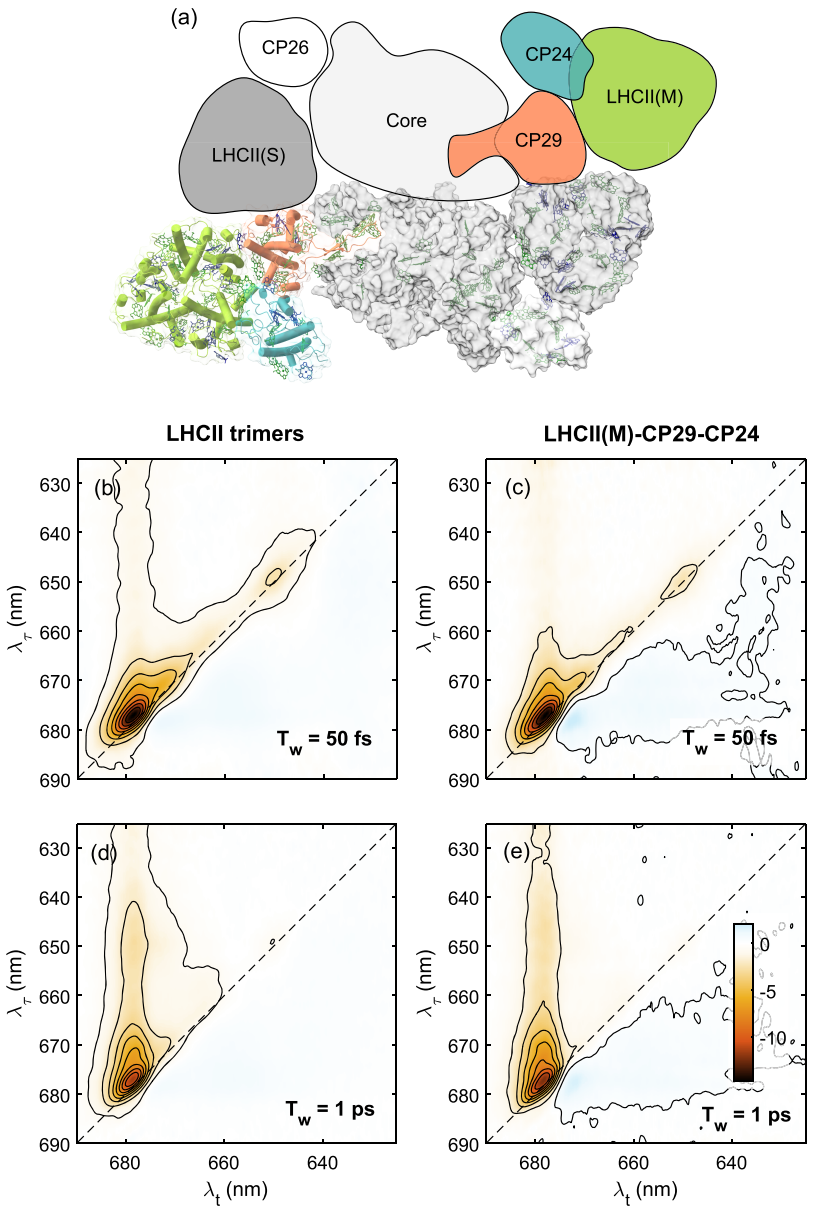

Figure 1. (a) Arrangement of subunits in the dimeric $C_2S_2M_2$-type PSII-SC from a 3.2 Å cryo-electron microscopic structure (PDB code 5XNM). The core, LHCII(S), LHCII(M), CP29, CP24, and CP26 are colored as gray, dark gray, light green, orange, teal, and white, respectively. The top half of the dimer is represented with the subunit schematic arrangements, mirroring the bottom half of the dimer, with a more detailed depiction with the polypeptide chains of the LHCII(M)−CP29−CP24 complex overlaid and colored. Chls *a* and *b* are plotted as green and blue sticks, respectively. (b−e) Representative 2D spectra at denoted waiting times T_w = 50 fs and 1 ps of LHCII and the M−CP_2 complex.

representative for a more asymmetric and native assembled form of LHCII. In contrast to the "bulk" solubilized LHCII trimers (henceforth simply called LHCII) that are a mixture of different combinations of Lhcb1−3 proteins, LHCII(M) in the M−CP_2 complex is a heterotrimer formed by two Lhcb1 units and one Lhcb3 unit. The largest Lhcb3 unit is associated strongly with the CP24−CP29 dimer.[5] A recently published structure of a $C_2S_2M_2$-type PSII−LHCII supercomplex with near-atomic resolution obtained by cryo-electron microscopy (cryo-EM) reveals many closely located Chls, which can serve as good candidates for the intercomplex EET processes.[5,6] Within the M−CP_2 complex, several EET pathways have been proposed, mainly from CP24 and LHCII(M) to CP29 as a result of the location of CP29 bridging the peripheral antennas to the PSII core region. Also proposed on the basis of structural evidence are additional intercomplex transfers involving Chl *b*, including an uphill EET from Chl $a614_{LHCII(M)}$ → Chl $b614_{CP29}$.[6,33] We will however show this pathway to be not significant in our 2DES data presented later. Inefficient EET pathways are usually predicted by structure-based studies because they are purely based on the Mg−Mg distances below 20 Å, without taking into account the excitonic energy landscape.

To obtain a better understanding of the EET network, we compare the 2DES results from the M−CP_2 complex to that of the "bulk" LHCII trimer system. First, we will focus on a significant feature in LHCII EET measurements. The putative long-lived "bottleneck" state in LHCII absorbing at the intermediate region (660−670 nm, between Chl *a* and Chl *b* absorption peaks) has been measured to relax on a time scale of ∼4−6 ps[25,28,34] and has been hypothesized to affect PSII

https://doi.org/10.1021/acs.jpclett.2c00194
J. Phys. Chem. Lett. 2022, 13, 4263−4271

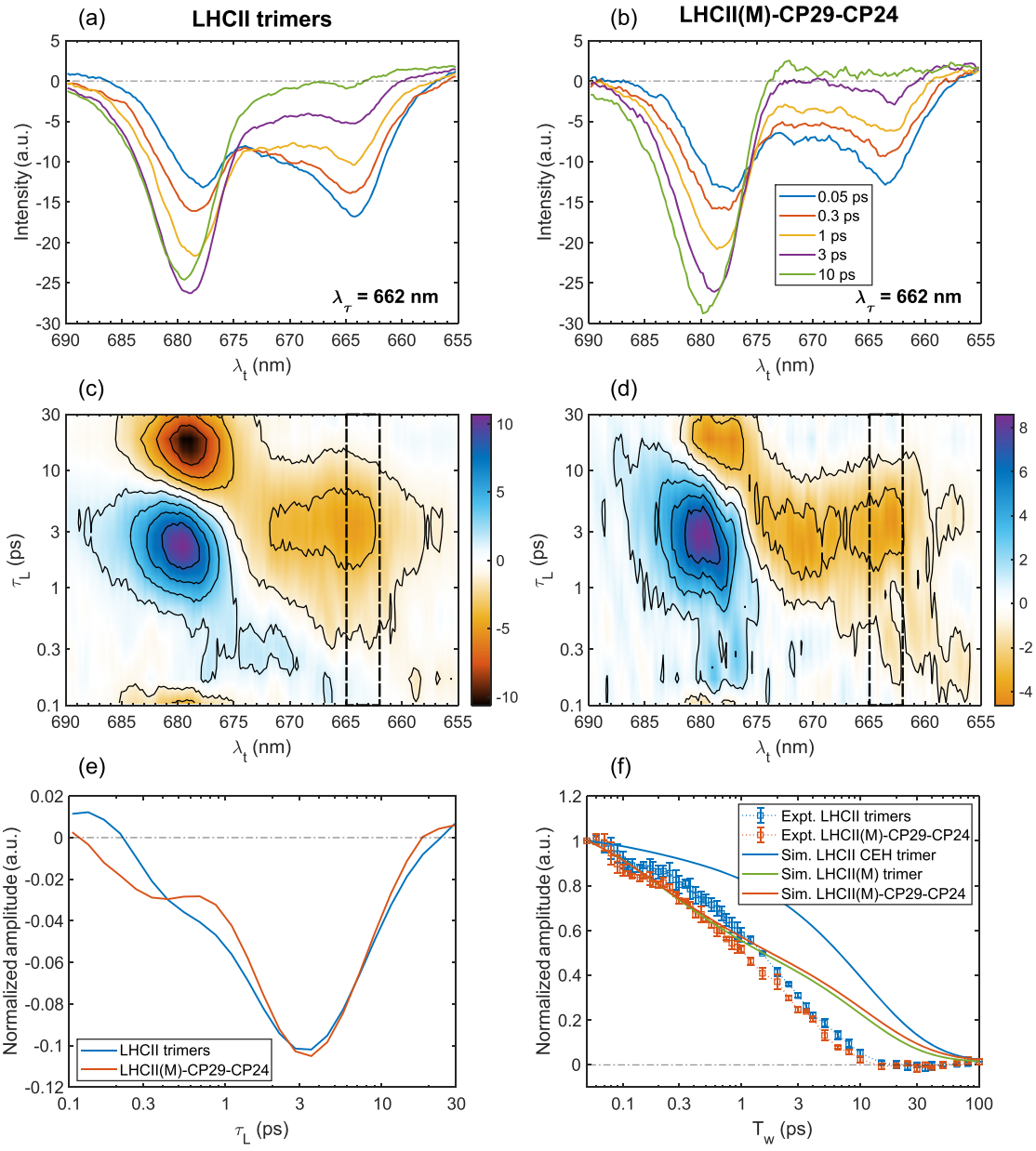

Figure 2. (a and b) Quasi-TA spectra obtained from integration of the 2D spectra of (a) LHCII and (b) M−CP_2 complex within ±1 nm around the denoted excitation wavelengths λ_τ = 662 at T_w from 50 fs to 10 ps. (c and d) 2D lifetime density map obtained from LDA at the excitation wavelength λ_τ = 662 nm. Black dashed boxes indicate the integration range of the 1D slices in panel e. (e) Normalized 1D traces along τ_L dimension highlight the lifetime distribution of the 662−665 nm bleach. (f) Kinetic traces obtained from the diagonal 662 nm signals of 2D spectra (squares) and corresponding simulated results from structure-based calculations (lines). The experimental data points are the mean ± standard deviation from three independent measurements. The experimental traces are integrated within ±2 nm around $(\lambda_\tau, \lambda_t)$ = (662, 664) nm, and simulated traces are integrated within 1 nm at $(\lambda_\tau, \lambda_t)$ = (658, 659) nm. The center difference is due to small deviations in simulated spectral peaks. All traces are normalized to the corresponding values at T_w = 50 fs. The error estimation details can be found in section S1 of the Supporting Information.

photodamage.[35] We will show that the "bottleneck" feature in LHCII(M) within M−CP_2 is diminished; i.e., the dynamics are sped up compared to LHCII. This dynamic difference can be explained by either the presence of intercomplex EET or structural differences between free trimeric LHCII and LHCII-(M) within the bigger aggregate. Furthermore, the additional dynamics contributed by CP24 and CP29 units will also need to be taken into consideration. These will be addressed in the subsequent analysis and discussions. Second, we will show that the Chl *b* dynamics are similar between the two complexes under study, implying that the intercomplex transfers involving Chl *b* mentioned earlier do not significantly alter the EET network.

Panels b and c of Figure 1 present the two-dimensional (2D) spectra at the early waiting time T_w = 50 fs of LHCII (solubilized trimer) and M−CP_2, respectively. The excitation spectral dependence has been corrected by dividing the 2D spectra with the corresponding laser excitation spectrum along the λ_τ dimension.[36] A 2D spectrum can be interpreted as a 2D frequency correlation map plotting the conditional population detected along the detection wavelength λ_t upon the initial excitation at wavelength λ_τ after a delay time T_w. The 2D spectra of the two complexes under study share some broadly similar features. The 2D spectra of both complexes at T_w = 50 fs show four diagonal features at around 650, 662, 670, and 678 nm,

https://doi.org/10.1021/acs.jpclett.2c00194
J. Phys. Chem. Lett. 2022, 13, 4263−4271

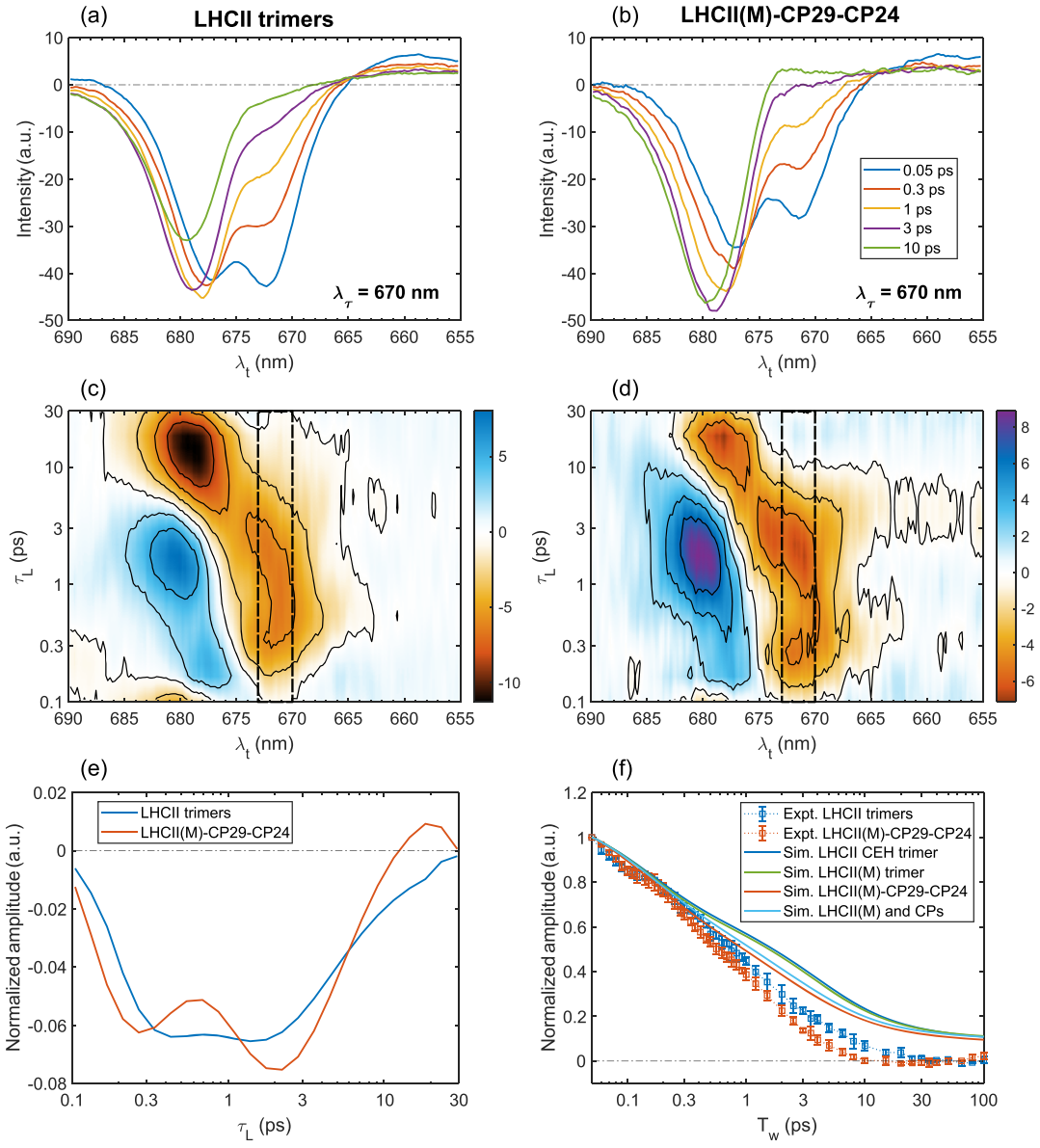

Figure 3. (a and b) Quasi-TA spectra, (c and d) 2D lifetime density map taken, and (e and f) kinetic comparison at λ_τ = 670 nm between the two complexes under study. The presentation is the same as Figure 2. The experimental traces are integrated within ±2 nm around $(\lambda_\tau, \lambda_t)$ = (670, 672) nm, and simulated traces are integrated within ±1 nm at $(\lambda_\tau, \lambda_t)$ = (669, 670) nm.

corresponding to the four absorption peaks observed in the Q_y region (cf. Figure S1 of the Supporting Information). The 650 nm peak representing the Chl *b* manifold, and the intermediate 662 and 670 nm features will be important in the comparison of the EET dynamics between the two complexes. At a later time, the high-energy diagonal features (650−670 nm) gradually decrease with the corresponding rise of the off-diagonal peaks ($\lambda_t \approx$ 680 nm). This spectral evolution is characteristic of EET processes, reflecting the energy flow from the high-energy excitonic levels to the lower energy sinks. The 2D spectra at T_w = 1 ps shown in panels d and e of Figure 1 highlight the dynamic difference between the two complexes. The diagonal features at 662 and 670 nm are almost depleted in M−CP_2 but are still quite pronounced in the spectra of LHCII. These two spectral features, which reflect the so-called "bottleneck" state dynamics, are further investigated below.

In LHCII, the long-lived states in the intermediate region (660−670 nm) relax on a time scale of ∼4−6 ps.[25,28,34,37,38] We first study the states resolved in the 2D spectra (Figure 1) at the diagonal signals at $(\lambda_\tau, \lambda_t)$ = (662, 664) nm. The quasi-transient absorption (TA) spectra for λ_τ = 662 nm in panels a and b of Figure 2 reveal differences in the EET dynamics of this spectral region between LHCII and M−CP_2. Lifetime density analysis (LDA; details in the Supporting Information) is performed on all independent measurements, and only the reproduceable features of LDA are discussed below. The main decay time constant of the negative bleach at λ_t = 664 nm is determined to be ∼4 ps (see Figure 2e), which is in good agreement with previous studies. However, in the M−CP_2 complex, besides the 4 ps decay, there is an additional decay component revealed at sub-picoseconds. From the lifetime distribution in Figure 2e, the average lifetimes of the 662 nm levels in both complexes are determined as $\bar{\tau}_L = (\sum_i A_i \tau_{L_i}^{-1} / \sum_i A_i)^{-1}$, where A_i is the amplitude obtained from LDA of the 662 nm levels at the lifetime τ_{L_i}. $\bar{\tau}_L$ of the 662 nm level is 2.5 ps in LHCII and 1.2 ps in

https://doi.org/10.1021/acs.jpclett.2c00194
J. Phys. Chem. Lett. 2022, 13, 4263−4271

M−CP_2. These results emphasize that the putative "bottleneck" states measured at 662 nm in LHCII are diminished in the M−CP_2 complex. By the comparisons of the kinetic traces in Figure 2f, it can be seen that there is a statistically significant difference within the T_w range from 0.1 to 1 ps. The acceleration of 662 nm levels in M−CP_2 further affirms that the ∼10−20 ps long-lived "bottleneck" state in LHCII predicted by previous models[25,37−39] is not very realistic and even less so in the bigger antenna complexes.

To rationalize this observation in the M−CP_2 complex, where the slow-decaying states usually observed in LHCII have been accelerated, we perform structure-based dynamic simulation using the modified Redfield-generalized Förster theory including the intramolecular vibronic transitions as derived by Renger et al.[40] (details in the Supporting Information). This high-level calculation has been successfully applied to model the time-resolved TA, steady-state absorption, fluorescence, linear, and circular dichroism spectra of LHCII.[40,41] The calculations are performed with three LHCII trimers obtained by X-ray crystallography (PDB code 1RWT), which are called CEH, BFG, and DIJ trimers based on the name of the polypeptide chains,[42] the LHCII(M) trimer, and the M−CP_2 complex obtained from the 3.2 Å resolution cryo-EM map of the $C_2S_2M_2$-type PSII-SC (PDB code 5XNM).[5]

The calculation on the LHCII(M) trimer is used to test the hypothesis that the experimentally observed difference in dynamics between the two complexes is mainly due to the additional excitonic couplings/connections that bridge the LHCII(M) trimer with the two monomeric complexes. However, through the comparison between the simulation results of the LHCII(M) trimer and M−CP_2 complex (green and orange lines in Figure 2f), the decays of 660 nm diagonal signals are almost the same between two simulations. This result suggests that simply disconnecting the monomeric complexes from LHCII(M) in M−CP_2 cannot yield the slower dynamics, as observed in the experimental 2D spectra. Indeed, such a reductionistic picture may not be entirely adequate. It is known that spectroscopic signals, such as the excitonic circular dichroism spectra and fluorescence quantum yield, differ between LHCII samples in different environments[43,44] as well as different aggregates.[45] On the other hand, the dynamics calculated from the LHCII X-ray structures are significantly slower than the decay of M−CP_2 (cf. blue and orange lines in Figure 2f), with the main difference at the 0.3−3 ps time scale, which is in broad qualitative agreement with the experimental results. Note that the three X-ray crystal structures yield almost identical results; hence, only the result of the CEH trimer is presented. This finding correlates the acceleration of the ∼662−664 nm excitonic states with the structural distortion of LHCII in the bigger assembly. This structural effect can be due to the intrinsic Lhcb3 unit of the LHCII(M) trimer, which was shown to have some specific properties that are distinct compared to Lhcb1 and Lhcb2, such as shorter N-terminal sequence, pigment binding sites, and red-shifted fluorescence maximum.[46] Alternatively, the binding of the minor antennas can induce some distortion to the overall protein manifold of LHCII(M) trimer and change the overall dynamics. These two scenarios are difficult to distinguish because the LHCII(M) trimer cannot be easily purified. The assignment agrees with previous studies, suggesting that the energy equilibrations of LHCII and CP29 are changed depending upon the degree of aggregation.[27,47−51] The excitonic interactions between Chls in LHCII were found to be perturbed differently in various detergent solutions, and LHCII in a lipid system was determined to retain the most native state.[43,44]

In the quasi-TA spectra in panels a and b of Figure 2, besides the diagonal bleach at λ_t = 664 nm, there is a significant off-diagonal signal at λ_t = 668−674 nm, which also evolves differently between the two complexes. In LHCII, the off-diagonal feature at λ_t = 668−674 nm remains roughly constant until 1 ps and then slowly decays, whereas in the M−CP_2 complex, this decay begins at an earlier time. The accelerated decay of the state at 670−672 nm is even more evident comparing panels a and b of Figure 3. The diagonal bleach at 672 nm of both LHCII and M−CP_2 decreases ∼50% within 1 ps. This can be attributed to the ultrafast equilibration between strongly coupled Chl *a* in the complexes. However, after 1 ps, the dynamic in LHCII is significantly slower compared to the M−CP_2 complex.

The lifetime density maps taken at λ_τ = 670 nm in panels c and d of Figure 3 reveal complex dynamics following direct excitation of the congested Chl *a* manifold. The sub-picosecond features are ascribed to the equilibration between strongly coupled Chl *a* and followed by several picosecond EET dynamics. The integrated slices in Figure 3e highlight the contrast between the 670 nm dynamics of the two complexes. The presence of a shoulder at τ_L > 10 ps for LHCII (blue line) is indicative of the significantly slower decay compared to M−CP_2 (orange line), where there is an absence of this shoulder, whose dynamics are mostly faster than 10 ps. We can see that the two kinetic traces in Figure 3f have differences that are statistically significant, primarily for T_w = 3−10 ps, showing the slower decay of the 670 nm level of LHCII compared to M−CP_2. Average lifetimes of 670 nm states in both complexes are also calculated on the basis of the lifetime distribution in Figure 3e and yielded $\overline{\tau}_L$ = 0.6 and 0.5 ps for LHCII and M−CP_2, respectively. The average lifetimes of 670 nm levels are not quantitatively different between the two complexes. However, this is not surprising because, according to the kinetic traces, the major difference in dynamics appears beyond 1 ps. If we readjust the $\overline{\tau}_L$ calculations and only consider the >1 ps time scale, the average lifetimes of 670 nm states are 4.2 and 2.3 ps for LHCII and M−CP_2.

We focus now on the dynamics of the diagonal peak at ∼670 nm. In panels a and b of Figure 3, the signal at λ_t = 670−672 nm of LHCII drops 50% compared to ∼75% for the M−CP_2 complex from 1 to 3 ps. At 10 ps, there is still a noticeable signal for LHCII, contrasting with the almost completely depleted signal in the M−CP_2 complex. This indicates that the "bottleneck" is very much diminished in the M−CP_2 complex. This trend can be seen even clearer in the experimental traces in Figure 3f, where the M−CP_2 complex signal decays to the baseline by ∼10 ps. Those observations imply that the intramonomeric relaxation within the minor antennas (CP29 and CP24), regardless of how fast or even devoid of "bottleneck" states, cannot totally account for the faster dynamics of M−CP_2. The line of reasoning is that if we assume very fast CP29 and CP24 intracomplex dynamics and the LHCII(M) trimer in M−CP_2 behaves like it does in its isolated state, we should still see some population at ∼10 ps being retained in M−CP_2, albeit at about ∼60% of the amplitude of that of "bulk" LHCII (because LHCII contributes ∼60% of the number of Chl *a* in the M−CP_2 complex). Figure 4 shows a comparison of 60% of the LHCII signals versus M−CP_2 for the T_w = 3−50 ps region. It is clear from the data that the M−CP_2 signal does not contain any slow LHCII dynamic component. The observation and analysis presented implies that the faster EET dynamics in M−CP_2

https://doi.org/10.1021/acs.jpclett.2c00194
J. Phys. Chem. Lett. 2022, 13, 4263−4271

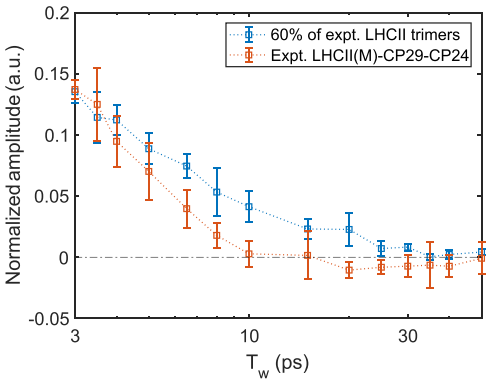

Figure 4. Comparison of two kinetic traces integrated within ±2 nm around $(\lambda_\tau, \lambda_t)$ = (670, 672) nm of 60% signals of LHCII and the M−CP_2 complex.

compared to LHCII at the 670 nm level cannot be fully accounted by only faster intramonomeric relaxation within the minor antennas (CP29 and CP24). In fact, intracomplex dynamics exhibiting a "bottleneck" of ∼3−5 ps lifetime are reported for CP29[52] and CP24,[53] similar to LHCII. This suggests that the intermonomeric transfer between LHCII(M) and the two CPs and/or structural distortion in the bigger assembly are needed to account for the observed dynamics.

To have an understanding to what extent the various factors can influence the 670 nm decay observed in M−CP_2, we compare the experimental and structure-based calculation results. We can see that the calculation predicts faster dynamics of 670 nm excitonic states in M−CP_2 compared to LHCII, and the amplitude difference is also qualitatively reproduced. However, the mechanism of the faster decay of the 670 nm states in M−CP_2 is not as clearly attributed as in the 662 nm region. In the 670 nm region, the calculation on LHCII(M)

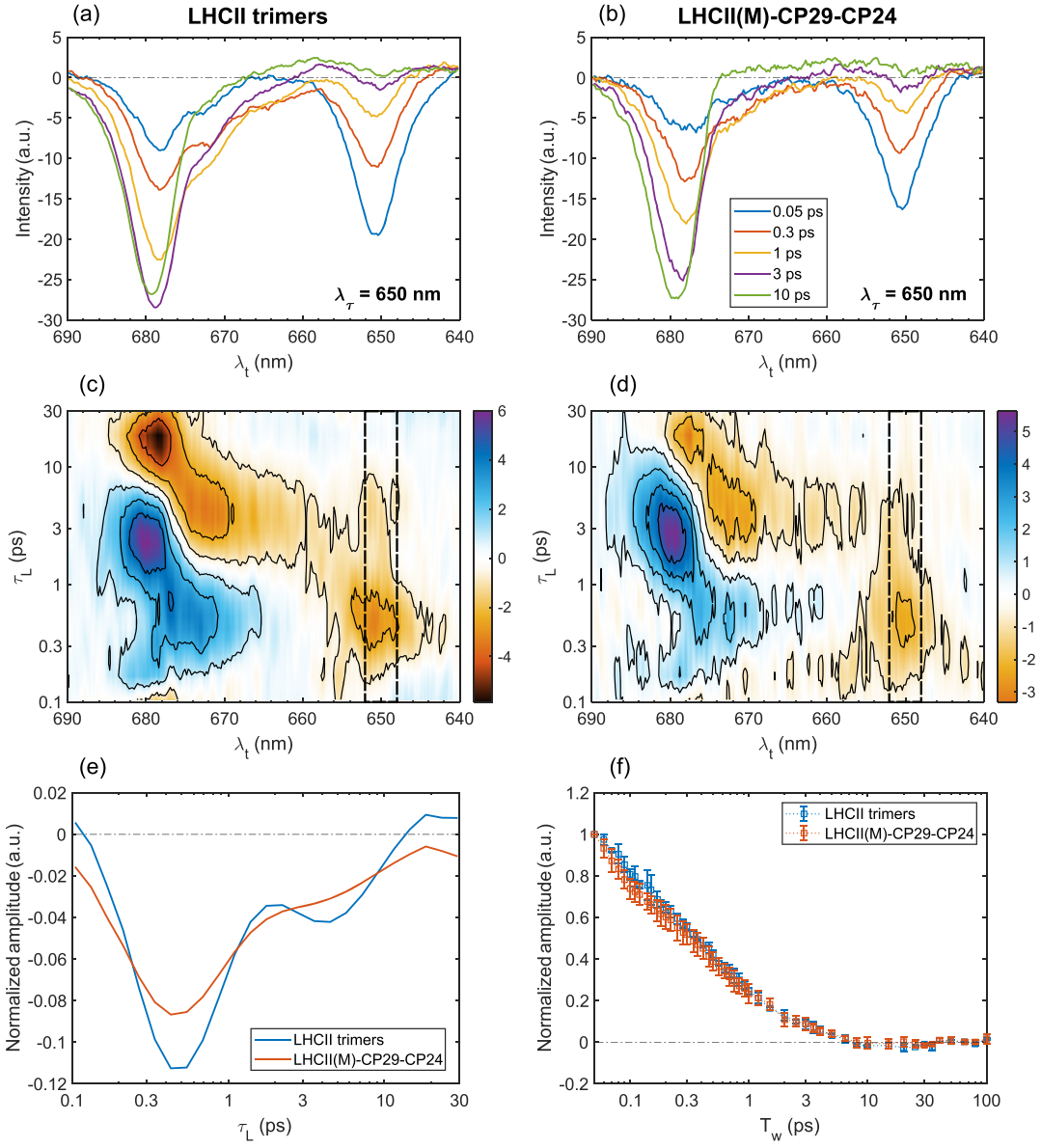

Figure 5. (a and b) Quasi-TA spectra, (c and d) 2D lifetime density map taken, and (e and f) kinetic comparison at λ_τ = 650 nm between the two complexes under study. The presentation is the same as Figure 2. The experimental kinetic traces are integrated within ±2 nm around $(\lambda_\tau, \lambda_t)$ = (650, 651) nm.

https://doi.org/10.1021/acs.jpclett.2c00194
J. Phys. Chem. Lett. 2022, 13, 4263−4271

yields a slower dynamic similar to the result of the LHCII CEH trimer. On the basis of this calculation result, it seems to suggest that the EET dynamic of the lower energy region of 670 nm is less sensitive to the structure distortion compared to the higher energy region of 662 nm. The structure-based simulation is then repeated with the M−CP_2 structure with all excitonic couplings between the LHCII(M) and two CPs removed; i.e., the intermonomeric transfers between LHCII(M) and CPs are effectively blocked, and the result is plotted in Figure 3f as the cyan line. According to the calculations, even with the intercomplex transfers blocked, the 670 nm signal still decays significantly faster than in LHCII trimers (with a slight slowdown as a result of some blocked EET pathways). These results suggest that the faster decay of 670 nm excitonic levels spectroscopically observed in M−CP_2 is partly due to the faster intracomplex EET dynamics at the 670 nm region of CP24 and CP29. To some extent, the intercomplex EETs may also contribute to the faster observed dynamics but cannot be the major factor, according to the structure-based calculations. Experiments on isolated CP29 indeed suggest higher contributions of sub-picosecond dynamics compared to LHCII,[52] which is probably due to the higher Chl *a*/*b* ratio of CP29 compared to the LHCII monomeric unit.[45] The structure-based calculation results also predict several fast intracomplex EET pathways within CP29, connecting the strongly coupled stromal Chl *a*, e.g., Chl *a*601−*a*602−*a*603−*a*611.

The Chl *b* manifold dynamics of the two complexes under study are compared in Figure 5. Panels a and b of Figure 5 show the quasi-TA spectra of Chl *b* excitation (λ_τ = 650 nm) of the two complexes. The negative bleach at λ_t = 650 nm, which represents the excited Chl *b* population, decays rapidly (∼70%) within 1 ps with the concomitant rise of the Chl *a* signals. After 1 ps, the decay of Chl *b* slows significantly and until 10 ps, and the negative bleach at λ_t = 650 nm is still slightly noticeable. The observed Chl *b* dynamics are in good agreement with several earlier studies reporting that the Chl *b* manifold in LHCII decays with the major time scale of 300 fs and a minor portion of long-lived population decays with a 3 ps lifetime.[14,25−27,54] The described kinetics are well-captured by the lifetime density maps presented in panels c and d of Figure 5. Integrated one-dimensional (1D) slices of both complexes around the diagonal region of 648−652 nm exhibit two main decay time constants: a major decay at ∼400 fs and another decay at ∼3−5 ps with a smaller amplitude. The kinetic traces shown in Figure 5f do not reveal any significantly different kinetics between LHCII and M−CP_2 within the noise level. We can infer from these experimental results that the intercomplex transfers bridging LHCII(M) and the two minor antennas suggested by structural studies[5,33] do not significantly alter the EET dynamics involving Chl *b*. This is in agreement with the theoretical derivation from Croce and van Amerongen that, as a result of the fast EET (sub-picosecond) pathways, the population of Chl *b* will be depleted mostly by intramonomeric EET before the intercomplex EET processes take place.[9] A recent 2DES study of LHCII oligomers trapped in lipid membrane nanodiscs reports an additional ultrafast 60 fs decay component for the Chl *b* beside the previously reported ∼300 fs decay dynamics.[55] The 60 fs decay is attributed to the strong intercomplex protein−protein interaction, although the exact mechanism remains unverified. As is apparent from our data, we do not see this extra sub-100 fs component in the M−CP_2 complex. This may imply that the distortion of the protein manifold and/or any structural changes that LHCII(M), CP29, and CP24 experience upon association in the M−CP_2 complex are not large enough to give rise to the additional ultrafast Chl *b* decay compared to oligomeric LHCII in nanodiscs (and presumably other aggregated forms).

In summary, the 2D spectra of M−CP_2 and LHCII obtained at 80 K are investigated, and the results reveal crucial differences in the exciton dynamics of these two types of complexes. The average lifetime of the states absorbing at 662−664 nm is shortened from 2.5 ps in LHCII to 1.2 ps in the M−CP_2 complex. The lower energy intermediate level at 670 nm also exhibits some acceleration at several picosecond time scale in M−CP_2. The acceleration effectively eliminates the "bottleneck" and shows that the LHCII EET dynamic is significantly altered in the bigger PSII-SC. The dynamics of the Chl *b* manifold are highly similar between LHCII and M−CP_2. Although this result was predicted previously by calculation,[9] in this study, we present the direct quantitative comparison to prove that, in the larger aggregate, the Chl *b* manifold in LHCII still mainly relaxes intramonomerically via sub-picosecond EET pathways.

The findings of this study open up interesting questions about light harvesting and EET dynamics in photosynthetic complexes. The measured differences between the EET dynamics of LHCII trimers and the LHCII(M)−CP29−CP24 complex suggest that the dynamics measured for complexes with a smaller set of components may not always be present or as dominant in the complexes with a larger set of components. These differences as we have observed cannot be simplistically explained solely by intercomplex EET processes but rather have to be analyzed holistically, with the structure of the larger complex in mind. The attribution to the structural influence further raises the question about the representative antenna size that should be used for light-harvesting functional studies. Given that the structure can have a major effect on the photosynthesis efficiency, the structure-based calculations need to be performed in suitable configurations, taking into consideration the cryogenic conditions of the published high-resolution structures to obtain more reliable predictions.

■ ASSOCIATED CONTENT

Supporting Information

The Supporting Information is available free of charge at https://pubs.acs.org/doi/10.1021/acs.jpclett.2c00194.

Descriptions about the experimental details (section S1), LDA (section S2), structure-based energy transfer dynamic simulation (section S3), and site energies and simulated 2D spectra (section S4) (PDF)

Transparent Peer Review report available (PDF)

■ AUTHOR INFORMATION

Corresponding Authors

Petar H. Lambrev − *Biological Research Center, Szeged, Szeged 6726, Hungary;* orcid.org/0000-0001-5147-153X; Email: lambrev.petar@brc.hu

Howe-Siang Tan − *Division of Chemistry and Biological Chemistry, School of Physical and Mathematical Sciences, Nanyang Technological University, Singapore 637371, Singapore;* orcid.org/0000-0003-2523-106X; Email: howesiang@ntu.edu.sg

Authors

Thanh Nhut Do − *Division of Chemistry and Biological Chemistry, School of Physical and Mathematical Sciences,*

https://doi.org/10.1021/acs.jpclett.2c00194
J. Phys. Chem. Lett. 2022, 13, 4263−4271

Nanyang Technological University, Singapore 637371, Singapore; orcid.org/0000-0002-5155-6936

Hoang Long Nguyen − *Division of Chemistry and Biological Chemistry, School of Physical and Mathematical Sciences, Nanyang Technological University, Singapore 637371, Singapore; Zernike Institute for Advanced Materials, University of Groningen, 9747 AG Groningen, Netherlands*

Parveen Akhtar − *Biological Research Center, Szeged, Szeged 6726, Hungary; ELI-ALPS, ELI-HU Nonprofit Limited, Szeged 6728, Hungary;* orcid.org/0000-0002-3264-7154

Kai Zhong − *Division of Chemistry and Biological Chemistry, School of Physical and Mathematical Sciences, Nanyang Technological University, Singapore 637371, Singapore; Zernike Institute for Advanced Materials, University of Groningen, 9747 AG Groningen, Netherlands*

Thomas L. C. Jansen − *Zernike Institute for Advanced Materials, University of Groningen, 9747 AG Groningen, Netherlands;* orcid.org/0000-0001-6066-6080

Jasper Knoester − *Zernike Institute for Advanced Materials, University of Groningen, 9747 AG Groningen, Netherlands*

Stefano Caffarri − *Aix Marseille Université, CEA, CNRS, BIAM, LGBP, 13009 Marseille, France*

Complete contact information is available at: https://pubs.acs.org/10.1021/acs.jpclett.2c00194

Notes

The authors declare no competing financial interest.

■ ACKNOWLEDGMENTS

This work was supported by grants from the Singapore Ministry of Education Academic Research Fund (Tier 1 RG2/19 and Tier 1 RG14/20 to Howe-Siang Tan), the National Research, Development and Innovations Office, Hungary (NKFIH 2018-1.2.1-NKP-2018-000009 to Petar H. Lambrev), and the Eötvös Loránd Research Network (KÖ-36/2021 to Petar H. Lambrev).

■ REFERENCES

(1) Barber, J. The engine of life: Photosystem II. *Biochemist* **2006**, *28* (4), 7−11.

(2) Caffarri, S.; Broess, K.; Croce, R.; van Amerongen, H. Excitation Energy Transfer and Trapping in Higher Plant Photosystem II Complexes with Different Antenna Sizes. *Biophys. J.* **2011**, *100* (9), 2094−2103.

(3) Caffarri, S.; Kouřil, R.; Kereïche, S.; Boekema, E. J.; Croce, R. Functional architecture of higher plant photosystem II supercomplexes. *EMBO J.* **2009**, *28* (19), 3052−3063.

(4) Crepin, A.; Santabarbara, S.; Caffarri, S. Biochemical and Spectroscopic Characterization of Highly Stable Photosystem II Supercomplexes from *Arabidopsis*. *J. Biol. Chem.* **2016**, *291* (36), 19157−19171.

(5) Su, X.; Ma, J.; Wei, X.; Cao, P.; Zhu, D.; Chang, W.; Liu, Z.; Zhang, X.; Li, M. Structure and assembly mechanism of plant C2S2M2-type PSII-LHCII supercomplex. *Science* **2017**, *357* (6353), 815−820.

(6) van Bezouwen, L. S.; Caffarri, S.; Kale, R. S.; Kouřil, R.; Thunnissen, A.-M. W. H.; Oostergetel, G. T.; Boekema, E. J. Subunit and chlorophyll organization of the plant photosystem II supercomplex. *Nat. Plants* **2017**, *3* (7), 17080.

(7) Wei, X.; Su, X.; Cao, P.; Liu, X.; Chang, W.; Li, M.; Zhang, X.; Liu, Z. Structure of spinach photosystem II−LHCII supercomplex at 3.2 Å resolution. *Nature* **2016**, *534* (7605), 69−74.

(8) Jansson, S. A guide to the Lhc genes and their relatives in *Arabidopsis*. *Trends Plant Sci.* **1999**, *4* (6), 236−240.

(9) Croce, R.; van Amerongen, H. Light harvesting in oxygenic photosynthesis: Structural biology meets spectroscopy. *Science* **2020**, *369* (6506), No. eaay2058.

(10) van Amerongen, H.; Croce, R. Structure and Function of Photosystem II Light-Harvesting Proteins (Lhcb) of Higher Plants. In *Primary Processes of Photosynthesis, Part 1: Principles and Apparatus*; Renger, G., Ed.; Royal Society of Chemistry: Cambridge, U.K., 2007; Chapter 8, pp 329−367, DOI: 10.1039/9781847558152-00329.

(11) Caffarri, S.; Croce, R.; Cattivelli, L.; Bassi, R. A Look within LHCII: Differential Analysis of the Lhcb1−3 Complexes Building the Major Trimeric Antenna Complex of Higher-Plant Photosynthesis. *Biochemistry* **2004**, *43* (29), 9467−9476.

(12) Betterle, N.; Ballottari, M.; Zorzan, S.; de Bianchi, S.; Cazzaniga, S.; Dall'Osto, L.; Morosinotto, T.; Bassi, R. Light-induced Dissociation of an Antenna Hetero-oligomer Is Needed for Non-photochemical Quenching Induction. *J. Biol. Chem.* **2009**, *284* (22), 15255−15266.

(13) Fuller, F. D.; Ogilvie, J. P. Experimental Implementations of Two-Dimensional Fourier Transform Electronic Spectroscopy. *Annu. Rev. Phys. Chem.* **2015**, *66*, 667−690.

(14) Lambrev, P. H.; Akhtar, P.; Tan, H.-S. Insights into the mechanisms and dynamics of energy transfer in plant light-harvesting complexes from two-dimensional electronic spectroscopy. *Biochim. Biophys. Acta, Bioenerg.* **2020**, *1861* (4), 148050.

(15) Schlau-Cohen, G. S.; Ishizaki, A.; Fleming, G. R. Two-dimensional electronic spectroscopy and photosynthesis: Fundamentals and applications to photosynthetic light-harvesting. *Chem. Phys.* **2011**, *386* (1−3), 1−22.

(16) Dostál, J.; Pšenčík, J.; Zigmantas, D. In situ mapping of the energy flow through the entire photosynthetic apparatus. *Nat. Chem.* **2016**, *8* (7), 705−710.

(17) Pan, J.; Gelzinis, A.; Chorošajev, V.; Vengris, M.; Senlik, S. S.; Shen, J.-R.; Valkunas, L.; Abramavicius, D.; Ogilvie, J. P. Ultrafast energy transfer within the photosystem II core complex. *Phys. Chem. Chem. Phys.* **2017**, *19* (23), 15356−15367.

(18) Myers, J. A.; Lewis, K. L. M.; Fuller, F. D.; Tekavec, P. F.; Yocum, C. F.; Ogilvie, J. P. Two-Dimensional Electronic Spectroscopy of the D1-D2-cyt b559 Photosystem II Reaction Center Complex. *J. Phys. Chem. Lett.* **2010**, *1* (19), 2774−2780.

(19) Gelzinis, A.; Abramavicius, D.; Ogilvie, J. P.; Valkunas, L. Spectroscopic properties of photosystem II reaction center revisited. *J. Chem. Phys.* **2017**, *147* (11), 115102.

(20) Lewis, K. L. M.; Fuller, F. D.; Myers, J. A.; Yocum, C. F.; Mukamel, S.; Abramavicius, D.; Ogilvie, J. P. Simulations of the Two-Dimensional Electronic Spectroscopy of the Photosystem II Reaction Center. *J. Phys. Chem. A* **2013**, *117* (1), 34−41.

(21) Duan, H.-G.; Prokhorenko, V. I.; Wientjes, E.; Croce, R.; Thorwart, M.; Miller, R. J. D. Primary Charge Separation in the Photosystem II Reaction Center Revealed by a Global Analysis of the Two-dimensional Electronic Spectra. *Sci. Rep.* **2017**, *7* (1), 12347.

(22) Fuller, F. D.; Pan, J.; Gelzinis, A.; Butkus, V.; Senlik, S. S.; Wilcox, D. E.; Yocum, C. F.; Valkunas, L.; Abramavicius, D.; Ogilvie, J. P. Vibronic coherence in oxygenic photosynthesis. *Nat. Chem.* **2014**, *6* (8), 706−711.

(23) Romero, E.; Augulis, R.; Novoderezhkin, V. I.; Ferretti, M.; Thieme, J.; Zigmantas, D.; van Grondelle, R. Quantum coherence in photosynthesis for efficient solar-energy conversion. *Nat. Phys.* **2014**, *10* (9), 676−682.

(24) Calhoun, T. R.; Ginsberg, N. S.; Schlau-Cohen, G. S.; Cheng, Y. C.; Ballottari, M.; Bassi, R.; Fleming, G. R. Quantum Coherence Enabled Determination of the Energy Landscape in Light-Harvesting Complex II. *J. Phys. Chem. B* **2009**, *113* (51), 16291−16295.

(25) Schlau-Cohen, G. S.; Calhoun, T. R.; Ginsberg, N. S.; Read, E. L.; Ballottari, M.; Bassi, R.; van Grondelle, R.; Fleming, G. R. Pathways of Energy Flow in LHCII from Two-Dimensional Electronic Spectroscopy. *J. Phys. Chem. B* **2009**, *113* (46), 15352−15363.

(26) Duan, H.-G.; Stevens, A. L.; Nalbach, P.; Thorwart, M.; Prokhorenko, V. I.; Miller, R. J. D. Two-Dimensional Electronic Spectroscopy of Light-Harvesting Complex II at Ambient Temperature: A Joint Experimental and Theoretical Study. *J. Phys. Chem. B* **2015**, *119* (36), 12017−12027.

(27) Enriquez, M. M.; Akhtar, P.; Zhang, C.; Garab, G.; Lambrev, P. H.; Tan, H.-S. Energy transfer dynamics in trimers and aggregates of

light-harvesting complex II probed by 2D electronic spectroscopy. *J. Chem. Phys.* **2015**, *142* (21), 212432.
(28) Akhtar, P.; Do, T. N.; Nowakowski, P. J.; Huerta-Viga, A.; Khyasudeen, M. F.; Lambrev, P. H.; Tan, H.-S. Temperature Dependence of the Energy Transfer in LHCII Studied by Two-Dimensional Electronic Spectroscopy. *J. Phys. Chem. B* **2019**, *123* (31), 6765−6775.
(29) Akhtar, P.; Zhang, C.; Do, T. N.; Garab, G.; Lambrev, P. H.; Tan, H.-S. Two-Dimensional Spectroscopy of Chlorophyll a Excited-State Equilibration in Light-Harvesting Complex II. *J. Phys. Chem. Lett.* **2017**, *8* (1), 257−263.
(30) Arsenault, E. A.; Yoneda, Y.; Iwai, M.; Niyogi, K. K.; Fleming, G. R. The role of mixed vibronic Q_y-Q_x states in green light absorption of light-harvesting complex II. *Nat. Commun.* **2020**, *11* (1), 6011.
(31) Ramanan, C.; Ferretti, M.; van Roon, H.; Novoderezhkin, V. I.; van Grondelle, R. Evidence for coherent mixing of excited and charge-transfer states in the major plant light-harvesting antenna, LHCII. *Phys. Chem. Chem. Phys.* **2017**, *19* (34), 22877−22886.
(32) Ginsberg, N. S.; Davis, J. A.; Ballottari, M.; Cheng, Y. C.; Bassi, R.; Fleming, G. R. Solving structure in the CP29 light harvesting complex with polarization-phased 2D electronic spectroscopy. *Proc. Natl. Acad. Sci. U. S. A.* **2011**, *108* (10), 3848−3853.
(33) Cao, P.; Su, X.; Pan, X.; Liu, Z.; Chang, W.; Li, M. Structure, assembly and energy transfer of plant photosystem II supercomplex. *Biochim. Biophys. Acta, Bioenerg.* **2018**, *1859* (9), 633−644.
(34) Do, T. N.; Huerta-Viga, A.; Akhtar, P.; Nguyen, H. L.; Nowakowski, P. J.; Khyasudeen, M. F.; Lambrev, P. H.; Tan, H.-S. Revealing the excitation energy transfer network of Light-Harvesting Complex II by a phenomenological analysis of two-dimensional electronic spectra at 77 K. *J. Chem. Phys.* **2019**, *151* (20), 205101.
(35) Ware, M. A.; Dall'Osto, L.; Ruban, A. V. An *In Vivo* Quantitative Comparison of Photoprotection in *Arabidopsis* Xanthophyll Mutants. *Front. Plant Sci.* **2016**, *7*, 841.
(36) Do, T. N.; Gelin, M. F.; Tan, H.-S. Simplified expressions that incorporate finite pulse effects into coherent two-dimensional optical spectra. *J. Chem. Phys.* **2017**, *147* (14), 144103.
(37) Novoderezhkin, V.; Salverda, J. M.; van Amerongen, H.; van Grondelle, R. Exciton modeling of energy-transfer dynamics in the LHCII complex of higher plants: A redfield theory approach. *J. Phys. Chem. B* **2003**, *107* (8), 1893−1912.
(38) Novoderezhkin, V. I.; Palacios, M. A.; van Amerongen, H.; van Grondelle, R. Excitation dynamics in the LHCII complex of higher plants: Modeling based on the 2.72 angstrom crystal structure. *J. Phys. Chem. B* **2005**, *109* (20), 10493−10504.
(39) Novoderezhkin, V. I.; van Grondelle, R. Physical origins and models of energy transfer in photosynthetic light-harvesting. *Phys. Chem. Chem. Phys.* **2010**, *12* (27), 7352−7365.
(40) Renger, T.; Madjet, M. E.; Knorr, A.; Müh, F. How the molecular structure determines the flow of excitation energy in plant light-harvesting complex II. *J. Plant Physiol.* **2011**, *168* (12), 1497−1509.
(41) Müh, F.; Renger, T. Refined structure-based simulation of plant light-harvesting complex II: Linear optical spectra of trimers and aggregates. *Biochim. Biophys. Acta, Bioenerg.* **2012**, *1817* (8), 1446−1460.
(42) Liu, Z. F.; Yan, H. C.; Wang, K. B.; Kuang, T. Y.; Zhang, J. P.; Gui, L. L.; An, X. M.; Chang, W. R. Crystal structure of spinach major light-harvesting complex at 2.72 angstrom resolution. *Nature* **2004**, *428* (6980), 287−292.
(43) Akhtar, P.; Dorogi, M.; Pawlak, K.; Kovács, L.; Bóta, A.; Kiss, T.; Garab, G.; Lambrev, P. H. Pigment Interactions in Light-harvesting Complex II in Different Molecular Environments. *J. Biol. Chem.* **2015**, *290* (8), 4877−4886.
(44) Li, F.; Liu, C.; Streckaite, S.; Yang, C.; Xu, P.; Llansola-Portoles, M. J.; Ilioaia, C.; Pascal, A. A.; Croce, R.; Robert, B. A new, unquenched intermediate of LHCII. *J. Biol. Chem.* **2021**, *296*, 100322.
(45) Xu, P.; Roy, L. M.; Croce, R. Functional organization of photosystem II antenna complexes: CP29 under the spotlight. *Biochim. Biophys. Acta, Bioenerg.* **2017**, *1858* (10), 815−822.
(46) Crepin, A.; Caffarri, S. Functions and Evolution of Lhcb Isoforms Composing LHCII, the Major Light Harvesting Complex of Photosystem II of Green Eukaryotic Organisms. *Curr. Protein Pept. Sci.* **2018**, *19* (7), 699−713.
(47) Simidjiev, I.; Barzda, V.; Mustárdy, L.; Garab, G. Isolation of Lamellar Aggregates of the Light-Harvesting Chlorophyll a/b Protein Complex of Photosystem II with Long-Range Chiral Order and Structural Flexibility. *Anal. Biochem.* **1997**, *250* (2), 169−175.
(48) Barzda, V.; Gulbinas, V.; Kananavicius, R.; Cervinskas, V.; van Amerongen, H.; van Grondelle, R.; Valkunas, L. Singlet−Singlet Annihilation Kinetics in Aggregates and Trimers of LHCII. *Biophys. J.* **2001**, *80* (5), 2409−2421.
(49) Barros, T.; Royant, A.; Standfuss, J.; Dreuw, A.; Kühlbrandt, W. Crystal structure of plant light-harvesting complex shows the active, energy-transmitting state. *EMBO J.* **2009**, *28* (3), 298−306.
(50) Chmeliov, J.; Gelzinis, A.; Songaila, E.; Augulis, R.; Duffy, C. D. P.; Ruban, A. V.; Valkunas, L. The nature of self-regulation in photosynthetic light-harvesting antenna. *Nat. Plants* **2016**, *2* (5), 16045.
(51) Mascoli, V.; Gelzinis, A.; Chmeliov, J.; Valkunas, L.; Croce, R. Light-harvesting complexes access analogue emissive states in different environments. *Chem. Sci.* **2020**, *11* (22), 5697−5709.
(52) Mascoli, V.; Novoderezhkin, V.; Liguori, N.; Xu, P.; Croce, R. Design principles of solar light harvesting in plants: Functional architecture of the monomeric antenna CP29. *Biochim. Biophys. Acta, Bioenerg.* **2020**, *1861* (3), 148156.
(53) Marin, A.; Passarini, F.; Croce, R.; van Grondelle, R. Energy Transfer Pathways in the CP24 and CP26 Antenna Complexes of Higher Plant Photosystem II: A Comparative Study. *Biophys. J.* **2010**, *99* (12), 4056−4065.
(54) Wells, K. L.; Lambrev, P. H.; Zhang, Z. Y.; Garab, G.; Tan, H.-S. Pathways of energy transfer in LHCII revealed by room-temperature 2D electronic spectroscopy. *Phys. Chem. Chem. Phys.* **2014**, *16* (23), 11640−11646.
(55) Son, M.; Moya, R.; Pinnola, A.; Bassi, R.; Schlau-Cohen, G. S. Protein−Protein Interactions Induce pH-Dependent and Zeaxanthin-Independent Photoprotection in the Plant Light-Harvesting Complex, LHCII. *J. Am. Chem. Soc.* **2021**, *143* (42), 17577−17586.

https://doi.org/10.1021/acs.jpclett.2c00194
J. Phys. Chem. Lett. 2022, 13, 4263−4271